



Hausdorff Distance with Outliers and Noise Resilience Capabilities

Baraka Jacob Maiseli¹

Received: 13 December 2020 / Accepted: 7 June 2021 / Published online: 26 June 2021
© The Author(s), under exclusive licence to Springer Nature Singapore Pte Ltd 2021

Abstract

For years, the Hausdorff distance (HD) has been an indispensable tool to address computer vision and pattern recognition problems. Compared with other metrics, HD incorporates critical details of objects (position and shapes) to output reasonable distances between pairs of point sets. Despite its capabilities, HD is highly sensitive to outliers and noisy data. From previous studies, we discovered that the issues have been inadequately addressed. In the present work, a technique is proposed to empower HD under undesirable conditions of data. The technique uses diffusion-like stopping kernels that investigate regions of data and trim-off outliers and noise. We, additionally, have analyzed our formulation to show why it works. Extensive experimental results demonstrate the efficacy of our approach relative to previous methods.

Keywords Hausdorff distance · Metric · Euclidean · Optimization · Point set

Introduction

Preliminaries

Distance refers to a numerical quantity that defines a theoretical/physical length between two objects. The quantity is useful to describe and measure a variety of phenomena: similarity of scenes, closeness of objects (cities, points, or sets), and irregularities in data. For instance, we can develop a convergence criterion in the evolving system to determine, at every iteration, how far the expected result is from the ideal one. The notion of distance is applied in almost all engineering and science disciplines [1–4].

A distance function (metric), f , on a set Ω is defined as $f : \Omega \times \Omega \rightarrow [0, \infty)$ and evaluates to a non-negative real number. Given that $a, b, c \in \Omega$, then f should satisfy the following axioms:

1. $f(a, b) \geq 0$, non-negativity or separation;
2. $f(a, b) = 0 \Leftrightarrow a = b$, identity of indiscernibles;
3. $f(a, b) = f(b, a)$, symmetry; and,

4. $f(a, c) \leq f(a, b) + f(b, c)$, subadditivity or triangle inequality.

One popular metric that obeys the mentioned axioms is based on the Euclidean space [1, 5–8], which measures the shortest route between points in a set. The Euclidean metric has an advantage of being isotropic, but it endures some irregularity properties that hinder its direct implementation in practical devices. Scholars have, therefore, attempted to address the challenge through alternative functions that produce reasonable approximations to the Euclidean metric. Typical non-Euclidean distances are Manhattan [9, 10], Chessboard [11], octagonal [12], quasi-Euclidean, and Hausdorff [13–18]. Our work is based on the Hausdorff distance (HD), which has captured a considerable attention of scholars over the past few decades [19–24].

Distance measures are widely applied in computer vision to determine the similarity between pairs of sets or images. For example, scholars have used HD in facial recognition to compare faces and templates stored in the databases [25–29]. Also, the Hausdorff distance find wide industrial applications in matching of the manufactured parts to isolate the defective ones.

One important necessity of a distance measure is robustness, which helps to deal with imperfections in the imaging process. Robust methods for distance measurements and comparisons can even be more valuable under natural environments where data suffer from noises, occlusions,

✉ Baraka Jacob Maiseli
barakaezra@udsm.ac.tz

¹ Department of Electronics and Telecommunications Engineering, College of Information and Communication Technologies, University of Dar es Salaam, 14113 Dar es Salaam, Tanzania

rotations, and translations. In this respect, therefore, robust versions of HD have been proposed [30–34]. The current work builds along this direction to establish a robust HD that can effectively deal with outliers and noise while retaining higher accuracy.

Motivations and Aims

Computing the distance between pairs of point sets is critical in several applications. Of interest is to apply a metric that is robust against outliers and noise, accurate, and efficient. The Hausdorff distance, commonly used in a range of computer vision and image processing tasks, may be regarded as an ideal choice to compute relatively more accurate distances between objects. Contrary to the notion of shortest distance, which collapses under situations of complex geometrical structures, HD considers relative position and complete shape of objects to compute the distance.

Despite the advantages, HD becomes seriously degraded in the presence of outliers and noisy data. A single erroneous datum in either set may lead to an overestimation of the distance value. Additionally, being directional, the Hausdorff distance violates the symmetry axiom. Because of these weaknesses, HD becomes unusable in most practical scenarios that involve corrupted and incomplete data. To deal with these undesirable conditions, plus situations of rotations and translations that the classical HD ignores, scholars have attempted to modify the measure [35–45]. Our analysis on these methods realized that the issues of extreme noise and outlier conditions have been inadequately discussed. Furthermore, some methods deviate significantly from the original Hausdorff distance even under normal conditions of the datasets [44].

Motivated by the challenges, we propose a robust Hausdorff distance (RHD) that integrates data-trimming functions to deal with noise and outliers. Experiments show that our approach produces promising results relative to other classical methods.

Contributions

The authors of this work have proposed a strategy that can increase the robustness of the traditional Hausdorff distance by rejecting outliers and noise in the point sets. Our method ensures that the Hausdorff distance maintains a higher accuracy under different conditions of data. We have, also, mathematically shown why the proposed approach works. Experimental results have been presented to backup and validate our claims regarding the superiority of the proposed method. We think that these contributions are useful and may further be extended to deal with hyperspaces and even more challenging point sets.

Hausdorff Distance

Let us consider two point sets, A and B , with elements $a \in A$ and $b \in B$. Then, the directed forward and backward Hausdorff distances between the sets are given by

$$h(A, B) = \max_{a \in A} \left\{ \min_{b \in B} f(a, b) \right\} \quad (1)$$

and

$$h(B, A) = \max_{b \in B} \left\{ \min_{a \in A} f(b, a) \right\}, \quad (2)$$

respectively. The HD is computed as

$$H(A, B) = \max \{ h(A, B), h(B, A) \}. \quad (3)$$

The values of $h(A, B)$ and $h(B, A)$ are not necessarily equal, and thus HD disobeys the symmetry axiom for certain types of datasets. The HD, in addition, overestimates distances under outlier environments. As a motivating example, let $A = \{17, 23\}$ and $B = \{25, 297\}$ (297 is apparently an outlier). Setting $f(a, b) = |a - b|$, we have $h(A, B) = 8$ and $h(B, A) = 274$; hence $H(A, B) = 274$, signaling the impact of the outlier. The next sections show an efficient approach to eliminate problematic data while emphasizing high accuracy of HD.

Robust Hausdorff Distance (RHD)

Problem Formulation

Our primary objective is to make the classical HD less sensitive to noise and outliers. To this end, and noting that overestimation of the HD is attributed to its $\max(\cdot)$ operator, we have introduced into the formulation two functions, $\phi(s)$ and $\psi(s)$, for locating and correcting discrepancies in the data. The variable s defines magnitude of the gradient: $s \rightarrow 0$ implies smooth data, and $s \rightarrow \infty$ signals corrupted data. Therefore, we define the forward and backward RHD between pairs of point sets, A and B , as

$$w(A, B) = \max_{a \in A} \left\{ \left(\min_{b \in B} f(a, b) \right) \circ \phi(s) \right\} \quad (4)$$

and

$$w(B, A) = \max_{b \in B} \left\{ \left(\min_{a \in A} f(b, a) \right) \circ \psi(s) \right\}, \quad (5)$$

respectively, where f defines a distance function and \circ is the Hadamard operator (element-wise multiplier between matrices). The outlier- and noise-suppressing functions, ϕ and ψ , should be monotonic with similar qualities (Fig. 1):

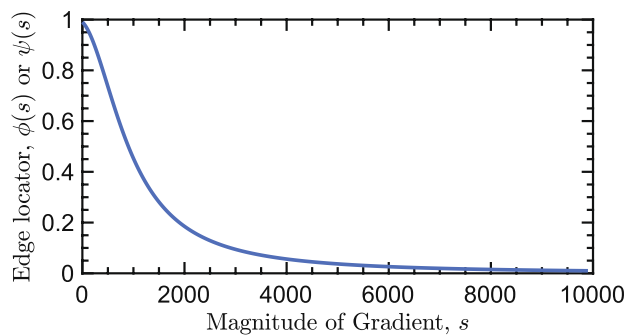


Fig. 1 Discrepancy-locating function

Table 1 Examples of discrepancy-locating functions, $\phi(s)$ or $\psi(s)$. K defines a thresholding parameter

| Type | $\phi(s)$ |
|--------------------|---|
| ℓ_1 | $\frac{1}{ s }$ |
| ℓ_2 | 1 |
| $\ell_1 - \ell_2$ | $\frac{1}{\sqrt{1 + \left(\frac{s}{K}\right)^2}}$ |
| Cauchy [48] | $\frac{1}{1 + \left(\frac{s}{K}\right)^2}$ |
| “Fair” [49] | $\frac{1}{1 + \frac{ s }{K}}$ |
| Geman-McClure [50] | $\frac{1}{(1+s^2)^2}$ |
| Welsch [51] | $\exp\left(-\left(\frac{s}{K}\right)^2\right)$ |
| Huber [52, 53] | $\begin{cases} 1 & \text{if } s \leq K \\ \frac{K}{ s } & \text{if } s \geq K \end{cases}$ |
| Tukey [54] | $\begin{cases} \left(1 - \left(\frac{s}{K}\right)^2\right)^2 & \text{if } s \leq K \\ 0 & \text{if } s > K \end{cases}$ |

$$\phi(s) = \begin{cases} 0 & \text{for } s \rightarrow \infty \\ 1 & \text{for } s \rightarrow 0 \end{cases} \quad (6)$$

Table 1 gives variants of $\phi(s)$ and $\psi(s)$ from robust statistics. The functionals

$$\phi\left(|\nabla(\min_{b \in B} f(a, b))|^2\right) = \frac{1}{1 + \left(\frac{|\nabla(\min_{b \in B} f(a, b))|}{K}\right)^2} \quad (7)$$

and

$$\psi\left(|\nabla(\min_{a \in A} f(b, a))|^2\right) = \frac{1}{1 + \left(\frac{|\nabla(\min_{a \in A} f(b, a))|}{K}\right)^2}, \quad (8)$$

where $K > 0$ is a thresholding parameter and ∇ represents gradient, have widely been reported in the literature that they give promising results in noise-suppression applications [46, 47]. The RHD is, therefore, given by

$$W(A, B) = \max(w(A, B), w(B, A)). \quad (9)$$

Why RHD Works?

Probably an intriguing question may be how ϕ and ψ in (7) and (8), respectively, make RHD robust. To explain the mechanics of our method, we consider a simple case of 1D point sets. When RHD is applied on the data, the discrepancy-locating functions inspect the sets to detect outliers, anomalous points present in the sets. Recalling (7) and (8), if the sets lack outliers then $\phi = 1$ and $\psi = 1$ because the difference between consecutive points, as defined by the ∇ operator, approaches zero. Our conception in this case is that absence of outliers in the datasets emulates smoothness, which can best be explained with a zero gradient. Therefore, (9) evaluates to a traditional Hausdorff distance. On the other hand, the presence of an outlier in either set makes the corresponding discrepancy-locating function zero because the gradients become high in the neighborhoods of the outlier (e.g., one-pixel width around the outlier). Consequently, erroneous entries are automatically rejected in both forward and backward operations of the Hausdorff distance—hence robustness of RHD.

For demonstration purposes, consider two point sets that contain real-valued elements: $A = \{a_1, a_2, \dots, a_M\}$ and $B = \{b_1, b_2, \dots, q, \dots, b_N\}$, where M and N are, respectively, cardinalities of A and B ; $a_i, b_j, q|_{j=1, \dots, N}^{i=1, \dots, M} \in \mathbb{R}^+$; $a_{i+1} > a_i$; and $q \gg b_{i+1} > b_i$, meaning that q is an extreme value (outlier or noise). For simplicity, let us further assume that $n(A \cap B) = 0$ (i.e., A and B are disjoint sets), $b_j > a_{i+1}$, and f is the absolute value function between pairs of entries in the sets:

$$f(a_i, b_j)|_{j=1, \dots, N}^{i=1, 2, \dots, M} = \begin{bmatrix} |a_1 - b_1| & |a_1 - b_2| & \dots & |a_1 - q| & \dots & |a_1 - b_N| \\ |a_2 - b_1| & |a_2 - b_2| & \dots & |a_2 - q| & \dots & |a_2 - b_N| \\ \vdots & \vdots & \ddots & \vdots & \ddots & \vdots \\ |a_i - b_1| & |a_i - b_2| & \dots & |a_i - q| & \dots & |a_i - b_N| \\ \vdots & \vdots & \ddots & \vdots & \ddots & \vdots \\ |a_M - b_1| & |a_M - b_2| & \dots & |a_M - q| & \dots & |a_M - b_N| \end{bmatrix} \quad (10)$$

and

$$f(b_j, a_i)_{j=1,2,\dots,N}^{i=1,2,\dots,M} = \begin{bmatrix} |b_1 - a_1| & |b_1 - a_2| & \dots & |b_1 - a_i| & \dots & |b_1 - a_M| \\ |b_2 - a_1| & |b_2 - a_2| & \dots & |b_2 - a_i| & \dots & |b_2 - a_M| \\ \vdots & \vdots & \vdots & \vdots & \vdots & \vdots \\ |q - a_1| & |q - a_2| & \dots & |q - a_i| & \dots & |q - a_M| \\ \vdots & \vdots & \vdots & \vdots & \vdots & \vdots \\ |b_N - a_1| & |b_N - a_2| & \dots & |b_N - a_i| & \dots & |b_N - a_M| \end{bmatrix}. \quad (11)$$

Therefore, considering the generalizations and assumptions, forward and backward distances of the traditional HD are respectively computed as

$$h(A, B) = \max_{a_i \in A} \left\{ \min_{b_j \in B} f(a_i, b_j) \right\} = \max_{a_i \in A} \begin{bmatrix} |a_1 - b_1| \\ |a_2 - b_1| \\ \vdots \\ |a_i - b_1| \\ \vdots \\ |a_M - b_1| \end{bmatrix} = |a_1 - b_1|, \text{ recalling the assumption that } a_{i+1} > a_i, \quad (12)$$

and

$$h(B, A) = \max_{b_j \in B} \left\{ \min_{a_i \in A} f(b_j, a_i) \right\} = \max_{b_j \in B} \begin{bmatrix} |b_1 - a_M| \\ |b_2 - a_M| \\ \vdots \\ |q - a_M| \\ \vdots \\ |b_N - a_M| \end{bmatrix} = |q - a_M|.$$

The M -element column vector in (12) emerges because, given the earlier assumptions, all first-column elements of the $M \times N$ matrix in (10) are lower than the corresponding elements in the other columns of the matrix. With this observation, the inner operation of the Hausdorff distance formula in (12), $\min_{b_j \in B} f(a_i, b_j)$, eliminates the high-value columns of $f(a_i, b_j)$. A similar reason holds for the derivation of (13) from (11).

Therefore, $H(A, B) = \max\{|a_1 - b_1|, |q - a_M|\} \approx q$, suggesting that HD is highly sensitive to outliers. Let us now consider our method:

$$w(A, B) = \max_{a_i \in A} \left\{ \min_{b_j \in B} f(a_i, b_j) \circ \phi(s) \right\}, \quad (14)$$

where

$$\phi(\cdot) = \begin{bmatrix} 1 \\ \frac{1}{1 + \left(\frac{|a_2 - b_1| - |a_1 - b_1|}{K} \right)^2} \\ \vdots \\ \frac{1}{1 + \left(\frac{|a_i - b_1| - |a_{i-1} - b_1|}{K} \right)^2} \\ \vdots \\ \frac{1}{1 + \left(\frac{|a_M - b_1| - |a_{M-1} - b_1|}{K} \right)^2} \end{bmatrix}, \text{ derived from (7);}$$

and,

$$w(B, A) = \max_{b_j \in B} \left\{ \min_{a_i \in A} f(b_j, a_i) \circ \psi(s) \right\}, \quad (15)$$

where

$$\psi(\cdot) = \begin{bmatrix} 1 \\ \frac{1}{1 + \left(\frac{|b_2 - a_M| - |b_1 - a_M|}{K} \right)^2} \\ \vdots \\ \frac{1}{1 + \left(\frac{|b_i - a_M| - |b_{i-1} - a_M|}{K} \right)^2} \\ \vdots \\ \frac{1}{1 + \left(\frac{|b_N - a_M| - |b_{N-1} - a_M|}{K} \right)^2} \end{bmatrix}, \text{ derived from (8).}$$

Plugging the definition of ϕ into (14) and that of ψ into (15), then evaluating the equations, we get

$$w(A, B) = \max_{a_i \in A} \begin{bmatrix} \frac{|a_1 - b_1|}{|a_2 - b_1|} \\ \frac{|a_2 - b_1|}{1 + \left(\frac{|a_2 - b_1| - |a_1 - b_1|}{K} \right)^2} \\ \vdots \\ \frac{|a_i - b_1|}{1 + \left(\frac{|a_i - b_1| - |a_{i-1} - b_1|}{K} \right)^2} \\ \vdots \\ \frac{|a_M - b_1|}{1 + \left(\frac{|a_M - b_1| - |a_{M-1} - b_1|}{K} \right)^2} \end{bmatrix} \approx |a_1 - b_1| \quad (16)$$

and

$$w(B, A) = \max_{b_j, q \in B} \left[\begin{array}{c} \frac{|b_1 - a_M|}{1 + \left(\frac{|b_2 - a_M| - |b_1 - a_M|}{K} \right)^2} \\ \vdots \\ \frac{|q - a_M|}{1 + \left(\frac{|q - a_M| - |b_j - a_M|}{K} \right)^2} \\ \vdots \\ \frac{|b_N - a_M|}{1 + \left(\frac{|b_N - a_M| - |b_{N-1} - a_M|}{K} \right)^2} \end{array} \right] \quad (17)$$

$$\approx \max_{b_j \in B} \left[\begin{array}{c} \frac{|b_1 - a_M|}{1 + \left(\frac{|b_2 - a_M| - |b_1 - a_M|}{K} \right)^2} \\ \vdots \\ \frac{|b_N - a_M|}{1 + \left(\frac{|b_N - a_M| - |b_{N-1} - a_M|}{K} \right)^2} \end{array} \right],$$

which signals an automatic rejection of an extreme datum, q , because $q \notin \{w(A, B), w(B, A)\}$. Furthermore, if K is carefully tuned (for instance, when $K = q$),

$$w(B, A) = |b_N - a_M| \left(\frac{1}{1 + \left(\frac{|b_N - a_M| - |b_{N-1} - a_M|}{K} \right)^2} \right) \approx |b_N - a_M| \quad (18)$$

and $W(A, B) = \max\{w(A, B), w(B, A)\} = \max\{|a_1 - b_1|, |b_N - a_M|\} = |b_N - a_M|$. This equation validates our hypothesis that the proposed method can effectively deal with erroneous data.

Experiments

Extensive range of experiments were conducted to test the efficacy of our method relative to some other classical distance measures. In the first experiment, we synthesized pairs of point sets and added an outlier to observe the discriminatory power of each method. Next, HD and RHD were applied to compute the distance between the sets. In the second experiment, point sets representing five types of scenes, namely Fish, Chinese characters, Elephant, Butterfly, Bird, and Chicken were downloaded from the public repository of test datasets¹ (Figs. 2, 3, 4, 5, 6 [55, 56]). Denoting these scenes from $i = 1, \dots, 6$ as the first pairs, A_i , the corresponding second pairs, B_i , were generated through transformation: $B_i = \Omega(\alpha_i \circ A_i) + t_i$, where α_i and t_i are the scaling factors and translation vectors, respectively, and $\Omega(\cdot)$ denotes the deformation function. We then applied HD and RHD on the pairs of datasets. To test for robustness, the experiment was repeated with the original scenes corrupted by outliers and random noise of density 1.50.

¹ <https://www.cise.ufl.edu/~anand/students/chui/tps-rpm.html>.

Table 2 Hausdorff distances under outlier conditions

| A | B | HD | MHD | Our method |
|-------|--------------|-------|-------|------------|
| 1.12 | 1.92 | 62.16 | 70.70 | 1.32* |
| 2.37 | 3.02 | | | |
| 3.19 | 3.92 | | | |
| 4.30 | 4.54 | | | |
| 5.92 | 6.72 | | | |
| 8.33 | 79.00 | | | |
| 10.78 | 11.27 | | | |
| 13.00 | 13.77 | | | |
| 14.73 | 15.02 | | | |
| 14.98 | 15.78 | | | |
| 16.84 | 17.43 | | | |

We also executed an experiment to compare our method and some other classical methods: MHD (modified HD) [44], RHD-FR (robust HD for face recognition) [30], and RHD-PS (robust HD using pyramidal structures) [34]. The objective of this experiment was to find a superior method that effectively deals with noise and outliers. For fair comparisons, parameters in the classical approaches were set for optimal results, and conditions of all experiments were maintained constant. We used the percentage relative error

$$\beta = \frac{|\varphi_1 - \varphi_o|}{\varphi_o} \times 100, \quad (19)$$

where φ_o and φ_1 are, respectively, the distances without and with outliers (and noise), as a performance evaluation metric.

Implementation codes for RHD have been shared in the MATLAB Central.²

Results and Discussions

Table 2 shows that the traditional Hausdorff distance is highly sensitive to outliers. From the table, removing an erroneous entry in B gives a distance of 1.3300 for both HD and our method, and 2.0490 for MHD. Including an outlier, however, causes HD and MHD to overestimate the distance while our method remains stable.

In scenes representing actual objects, RHD demonstrates compelling results under clean and noise-outlier conditions (Tables 3, 4, 5). The strength of our approach is attributed to the thresholding functions, ϕ and ψ , which encourage smoothness of data. In the presence of outliers, RHD creates

² <https://www.mathworks.com/matlabcentral/fileexchange/62082-robust-hausdorff-distance>.

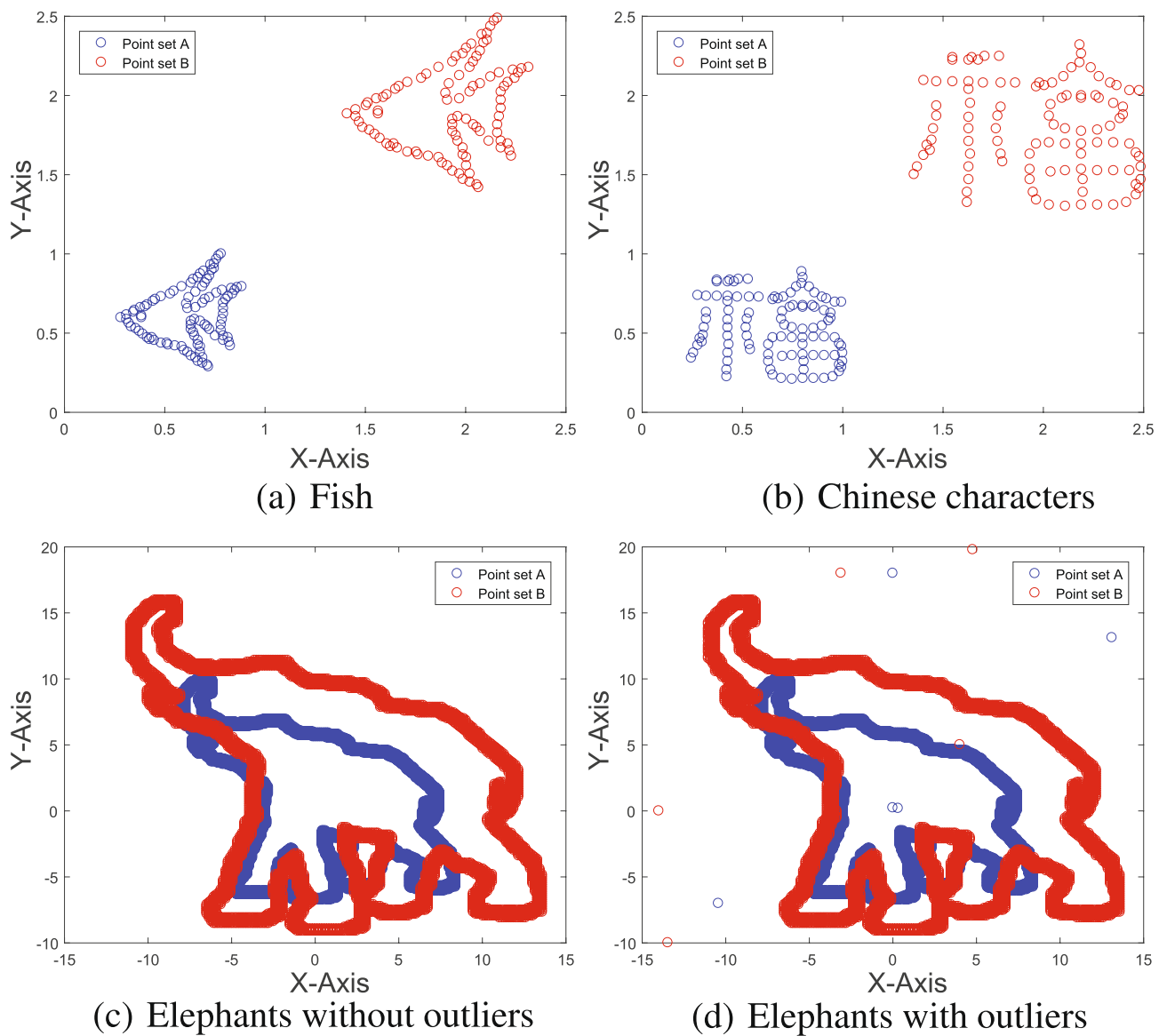


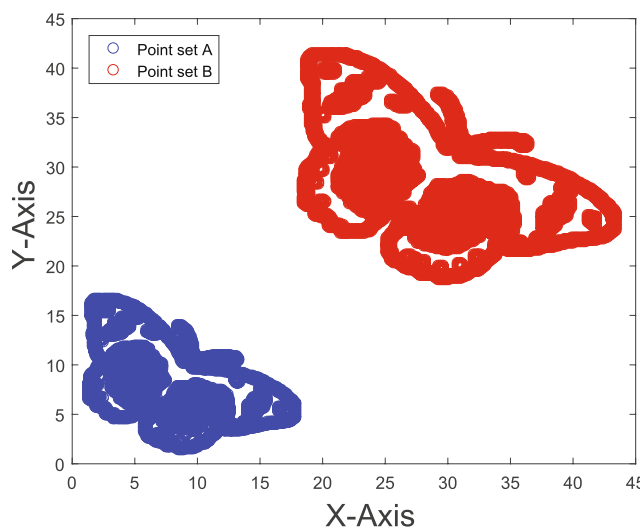
Fig. 2 Pairs of point sets

a negative potential around the ripples (outliers) to suppress the discrepancies. This way, the distance value is constrained within the acceptance ranges. On the contrary, the classical Hausdorff distance collapses under these harsh conditions, as demonstrated by the Tables. In particular 1D cases of datasets, as depicted by Table 2, even the modified Hausdorff distance by Dubuisson and Jain performs poorly whereas our method demonstrates a higher performance [44].

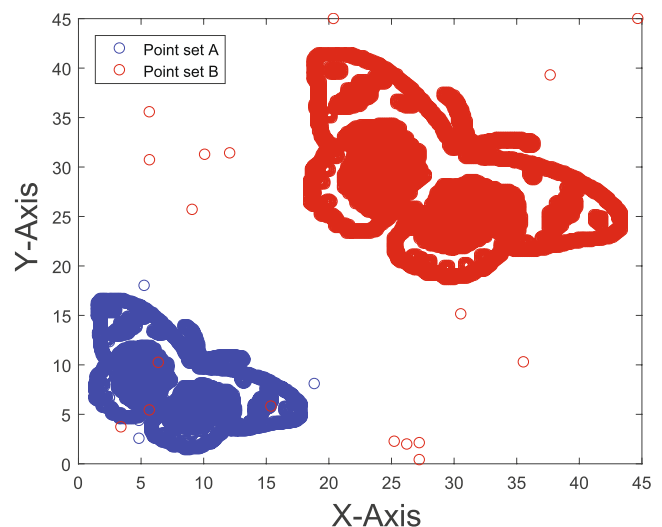
From Table 4, we can observe that the performance of our method is slightly lower than that of the modified Hausdorff distance. This observation suggests an interesting research avenue to further improve the proposed method in situations of deformed objects. One attempt to improve the method could be to modify the regularization kernels, ϕ and ψ , or

to incorporate a prior information (e.g., deformation matrix) into these kernels. Despite this limitation, our method generates outstanding results in objects with outliers, as depicted by Fig. 5b

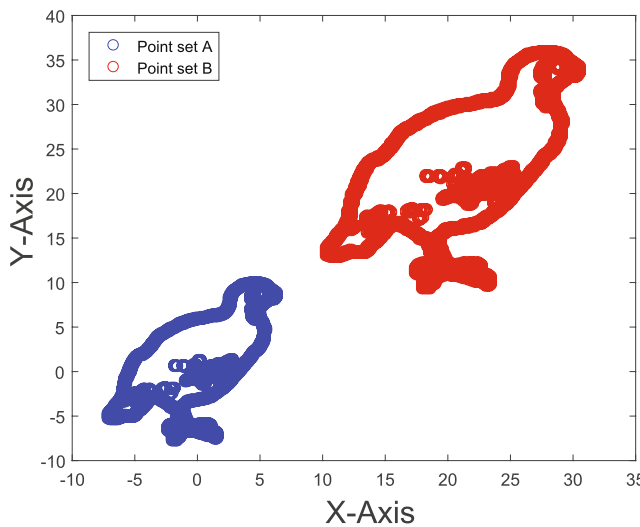
Figure 5b, d shows the deformed shapes of the Fish and Chinese characters, and Fig. 6 depicts a three-dimensional model of a chicken at different resolutions. The corresponding results in Table 4 suggest that our method outperforms the classical Hausdorff Distance in all cases. But MHD (modified version of the Hausdorff distance) slightly outperforms our method in two cases: deformed Chinese characters and chicken model. This observation was expected because the original conception of our method was based on outliers and noisy data—where it generates outstanding results. This



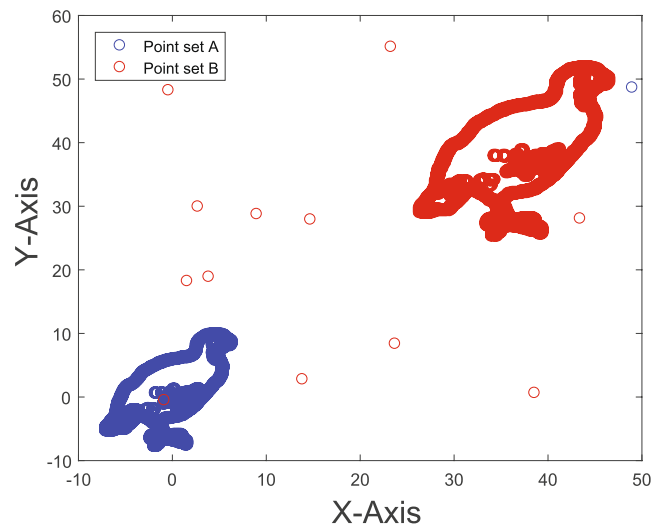
(a) Butterfly without outliers



(b) Butterfly with outliers



(c) Birds without outliers

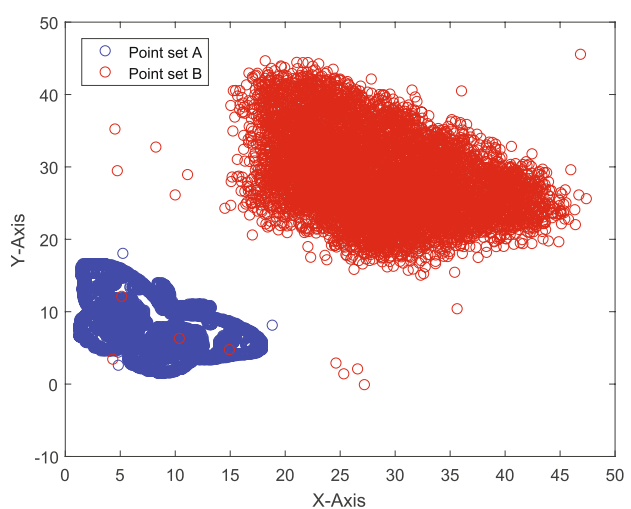


(d) Birds with outliers

Fig. 3 Pairs of point sets

limitation gives another interesting research avenue to incorporate other forms of prior knowledge, such as deformation matrices, into ϕ and ψ .

Despite some promising strengths of the proposed approach, the tuning constant K should be carefully selected to ensure a proper tradeoff between fidelity of results and data smoothness. From experiments, we found that $K = 3$ produces reasonable distances in various cases. But, a systematic procedure is needed to determine the value of K depending upon the nature and type of data. And, perhaps we need different values of K for both forward and backward Hausdorff distances. Determining the value of K manually is rather a challenging task. To automate the process, we

**Fig. 4** Pairs of point sets with outliers and noise

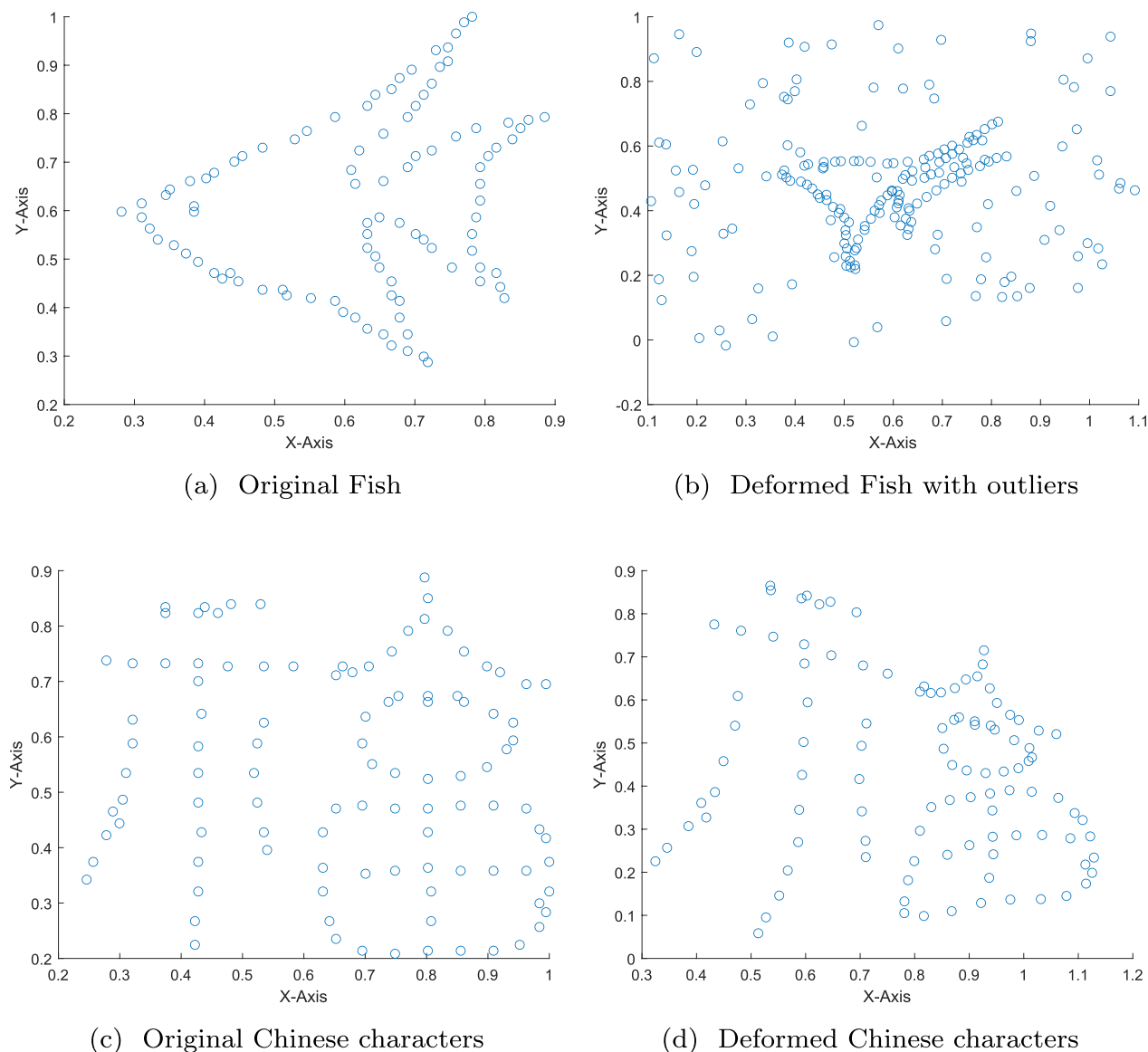


Fig. 5 Deformation of different model shapes

have proposed a simple iterative algorithm that computes the value of K at the lowest possible percentage error between the classical and the proposed Hausdorff distances (Fig. 7). Variation of percentage error with K is depicted by Fig. 8.

Selecting a suitable kernel (ϕ and ψ) is an important task to produce more accurate results. We recommend a kernel (weighing function) to be selected based on its ability to reject outliers. In essence, when such a kernel plugs into a diffusion equation, the resulting formulation should generate outstanding denoising results. In this work, we have used a kernel version similar to that used by Perona and Malik in their noise-suppressing diffusion framework [46]. This

kernel has been shown that it produces promising results, especially when it contains a properly designed tuning constant [47]. Nevertheless, superior and robust kernels, such as those exemplified in Table 1, should be explored to further improve our current findings.

The present work has considered one-, two-, and three-dimensional point sets, which are often encountered in a range of vision-related and pattern recognition tasks. Extending the study to high-order spaces may add some useful insights in the field. For instance, RHD may be extended and applied to compare and analyze multi-dimensional LIDAR (light detection and ranging) and medical images.

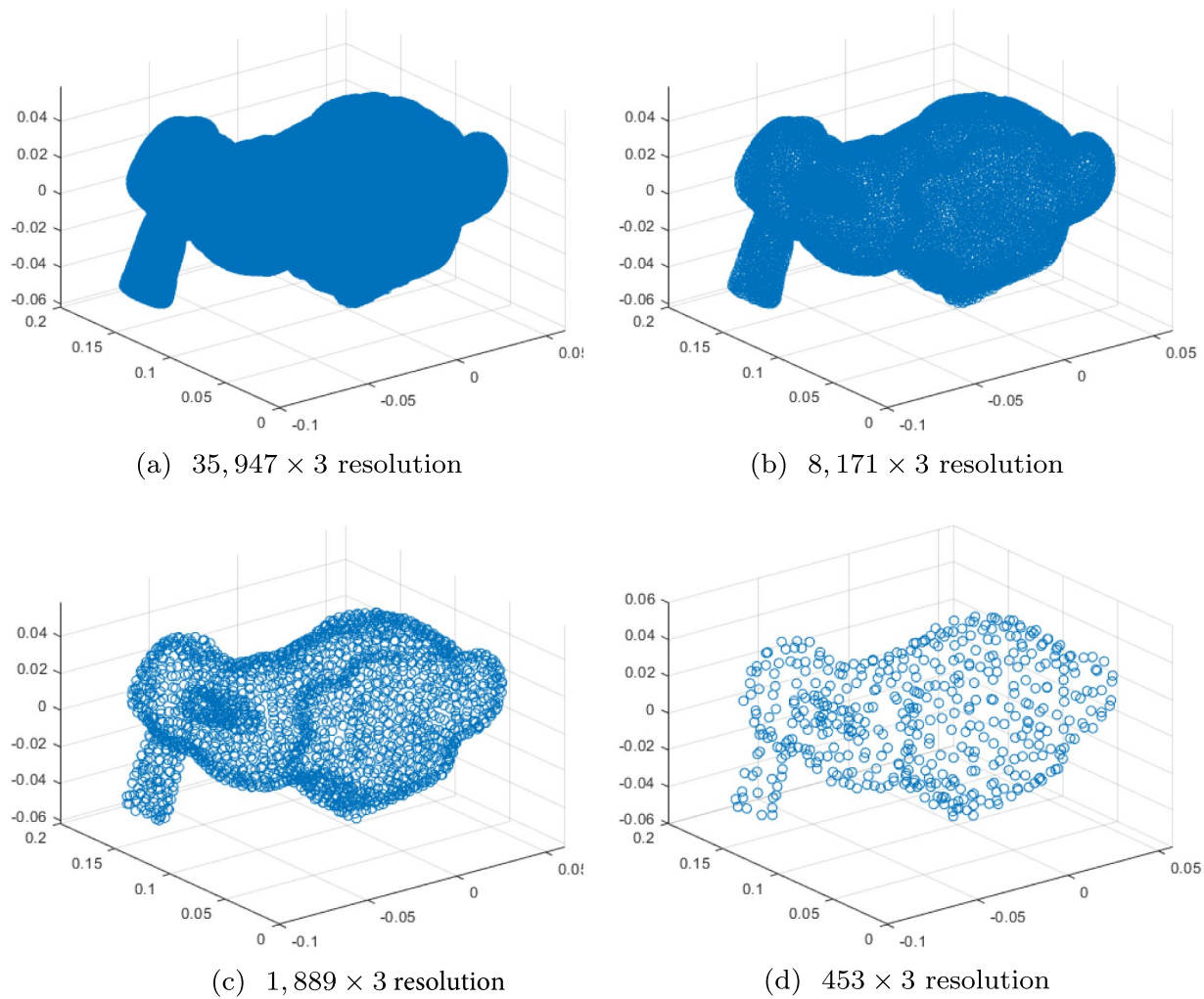
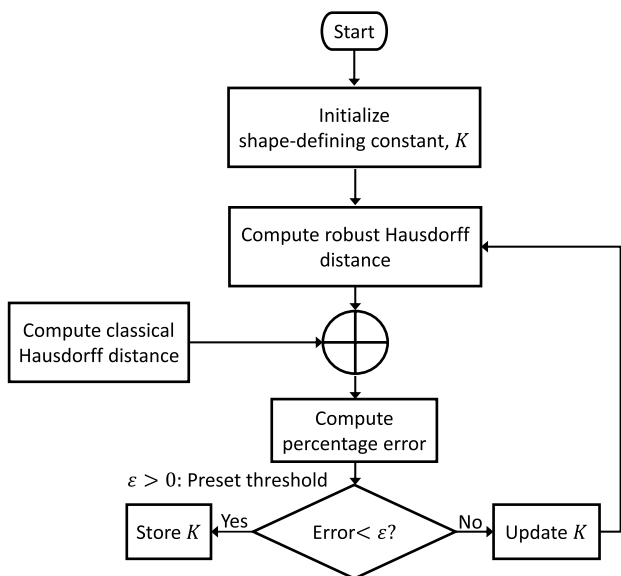
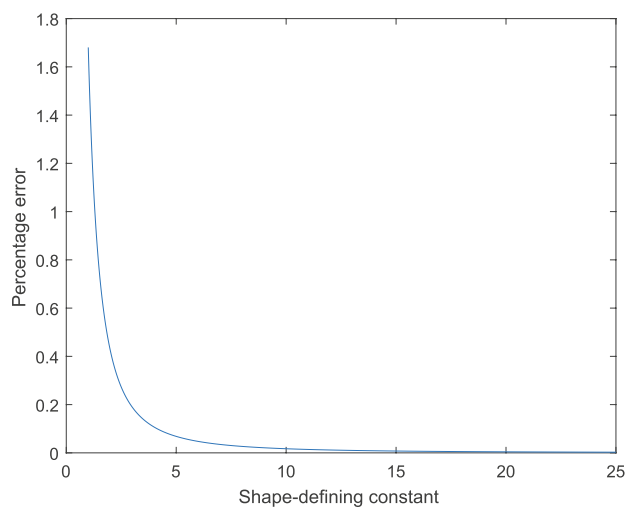
**Fig. 6** 3D model at different resolutions**Fig. 7** Computation of the shape-defining constant**Fig. 8** Percentage error versus shape-defining constant

Table 3 Classical (HD) and proposed (RHD) Hausdorff distances of different point sets of scenes

| Scene | No outliers | | Outliers | | Outliers + noise | |
|--------------------|-------------|---------|----------|---------|------------------|----------------|
| | HD | RHD | HD | RHD | HD | RHD |
| Fish | 2.0280 | 2.0280 | 47.4680 | 2.0280 | | |
| Chinese characters | 1.9969 | 1.9969 | 13.7861 | 2.0024 | | |
| Elephant | 6.4974 | 6.4974 | 7.8644 | 6.4958 | | |
| Butterfly | 32.1056 | 32.1056 | 45.0577 | 32.2437 | 46.7571 | 32.1036 |
| Bird | 35.1461 | 35.1459 | 38.5170 | 35.1018 | | |

Table 4 Hausdorff distances on deformed and sampled point sets

| | HD | MHD | RHD |
|----------------------------------|--------|--------|--------|
| Deformed Fish | 0.5053 | 0.1054 | 0.0339 |
| Deformed Chinese characters | 0.1894 | 0.0534 | 0.1451 |
| Chicken (35, 947 × 3 resolution) | 0.0023 | 0.0010 | 0.0019 |
| Chicken (8, 171 × 3 resolution) | 0.0050 | 0.0022 | 0.0041 |
| Chicken (1, 889 × 3 resolution) | 0.0100 | 0.0045 | 0.0091 |

Table 5 Hausdorff distances generated by various methods under outlier and noise conditions

| Scene | Percentage error (% error) | | | |
|--------------------|----------------------------|---------------|--------|---------------|
| | MHD | RHD-FR | RHD-PS | RHD |
| Fish | 45.3914 | 0.0912 | 0.0808 | 0.0000 |
| Chinese characters | 13.1270 | 2.0110 | 1.8912 | 0.2757 |
| Elephant | 0.0066 | 0.0050 | 0.0178 | 0.0242 |
| Butterfly-1 | 4.6697 | 2.0910 | 1.5409 | 0.4304 |
| Butterfly-2 | 4.5976 | 1.9979 | 0.7891 | 0.0060 |
| Bird | 10.4590 | 3.3320 | 1.4001 | 0.1254 |

Conclusion

We have modified a classical Hausdorff distance to deal with challenging datasets under noisy and outlier conditions. The proposed technique embeds a diffusion-like kernel that robustly rejects erroneous details in the data. Experimental results show that our approach generates reasonable distances compared with those from previous techniques. The proposed method may suit applications that involve point sets subjected to undesirable conditions. Future implementations may consider extending our approach to higher-dimensional data sets, including those generated for remote sensing and medical applications. In addition, the computational time $\mathcal{O}(m * n)$, with m and n representing the number of elements in the pairs of point sets, can further be reduced by learning the nature and patterns of the data sets, and then eliminating unwanted points before execution of our algorithm.

Declarations

Conflict of interest On behalf of all authors, the corresponding author states that there is no conflict of interest.

References

- Draisma J, Horobet E, Ottaviani G, Sturmfels B, Thomas RR. The Euclidean distance degree of an algebraic variety. *Found Comput Math*. 2016;16:99–149.
- Montecchesi L, Cocconcelli M, Rubini R. Artificial immune system via Euclidean distance minimization for anomaly detection in bearings. *Mech Syst Signal Process*. 2016;76:380–93.
- Mei X, Liu L, Prokhorov DV, Lu H. Collaborative distance metric learning for method and apparatus visual tracking, US Patent US9373036B1. U.S. Patent and Trademark Office, Washington, DC. 2016.
- Alvarez L, Cuenca C, Esclarín J, Mazorra L, Morel JM. Affine invariant distance using multiscale analysis. *J Math Imaging Vision*. 2016;55(2):199–209.
- Liberti L, Lavor C, Maculan N, Mucherino A. Euclidean distance geometry and applications. *SIAM Rev*. 2014;56:3–69.
- Kellmeyer P. Euclidean distance as a measure of ventral and dorsal white matter connectivity. 2016. <https://doi.org/10.1101/053959>.
- Wang J, Tan Y. Efficient Euclidean distance transform algorithm of binary images in arbitrary dimensions. *Pattern Recogn*. 2013;46:230–42.
- Xia S, Xiong Z, Luo Y, Zhang G, et al. Effectiveness of the Euclidean distance in high dimensional spaces. *Opt Int J Light Electron Opt*. 2015;126(24):5614–9.
- Jiang X, Hu X, He T. Identification of the clustering structure in microbiome data by density clustering on the Manhattan distance. *Sci China Inf Sci*. 2016;59(7):070104.
- Strauss T, von Maltitz MJ. Generalising ward's method for use with Manhattan distances. *PLoS One*. 2017;12:e0168288.
- Hari J, Prasad AS, Rao SK. Separation and counting of blood cells using geometrical features and distance transformed watershed. In: 2014 2nd International Conference on Devices, Circuits and Systems (ICDCS). IEEE, 2014. pp. 1–5. <https://doi.org/10.1109/ICDCSyst.2014.6926205>.
- Kaliamoorthi P, Kakarala R. Directional chamfer matching in 2.5 dimensions. *IEEE Signal Process Lett*. 2013;20(12):1151–4.
- Taha AA, Hanbury A. An efficient algorithm for calculating the exact Hausdorff distance. *IEEE Trans Pattern Anal Mach Intell*. 2015;37(11):2153–63.
- Gao Y, Wang M, Ji R, Wu X, Dai Q. 3-D object retrieval with Hausdorff distance learning. *IEEE Trans Ind Electron*. 2014;61(4):2088–98.

15. Wei Q, Liang X, Jiancheng F. A new star identification algorithm based on improved hausdorff distance for star sensors. *IEEE Trans Aerosp Electron Syst.* 2013;49(3):2101–9.
16. Sangineto E. Pose and expression independent facial landmark localization using dense-SURF and the Hausdorff distance. *IEEE Trans Pattern Anal Mach Intell.* 2013;35(3):624–38.
17. Wang JQ, Wu JT, Wang J, Zhang HY, Chen X. Multi-criteria decision-making methods based on the Hausdorff distance of hesitant fuzzy linguistic numbers. *Soft Comput.* 2016;20(4):1621–33.
18. Kyurkchiev N, Markov S. On the Hausdorff distance between the Heaviside step function and Verhulst logistic function. *J Math Chem.* 2016;54:109–19.
19. Wang C, Agarwal RP, O'Regan D, Sakthivel R. A computation method of Hausdorff distance for translation time scales. *Appl Anal.* 2018;99:1218–47. <https://doi.org/10.1080/00036811.2018.1529303>.
20. Ding S, Lin X, Zhang Z, Li Z, Chen L, Weng H. A novel Hausdorff distance based restrain criterion for zero-sequence differential protection of converter transformer. *Int J Electr Power Energy Syst.* 2019;105:753–64.
21. Sevakula RK, Verma NK. Hausdorff distance-based binary search tree multiclass decomposition algorithm. In: Computational intelligence: theories, applications and future directions, vol. II. Springer; 2019. pp. 239–49.
22. Kang Y, Yoon SH, Kyung MH, Kim MS. Fast and robust computation of the Hausdorff distance between triangle mesh and quad mesh for near-zero cases. *Comput Graph.* 2019;81:61–72. <https://doi.org/10.1016/j.cag.2019.03.014>.
23. He L, Tan H, Huang ZC. Online handwritten signature verification based on association of curvature and torsion feature with Hausdorff distance. *Multimedia Tools Appl.* 2019;78:19253–78.
24. Shmerkin P. On the Hausdorff dimension of pinned distance sets. *Isr J Math.* 2019;230(2):949–72.
25. Takacs B. Comparing face images using the modified Hausdorff distance. *Pattern Recogn.* 1998;31(12):1873–81.
26. Guo B, Lam KM, Lin KH, Siu WC. Human face recognition based on spatially weighted Hausdorff distance. *Pattern Recogn Lett.* 2003;24:499–507.
27. Lin KH, Lam KM, Siu WC. Spatially Eigen-weighted Hausdorff distances for human face recognition. *Pattern Recogn.* 2003;36(8):1827–34.
28. Achermann B, Bunke H. Classifying range images of human faces with Hausdorff distance. In: In: Proceedings 15th International Conference on Pattern Recognition. ICPR-2000, vol 2. IEEE, 2000. pp. 809–13. <https://doi.org/10.1109/ICPR.2000.906199>.
29. Jesorsky O, Kirchberg KJ, Frischholz RW. Robust face detection using the Hausdorff distance. In: Bigun J, Smeraldi F. (eds) Audio- and Video-Based Biometric Person Authentication. AVBPA 2001. Lecture Notes in Computer Science, vol 2091. Springer, Berlin, Heidelberg. https://doi.org/10.1007/3-540-45344-X_14.
30. Sudha N, et al. Robust Hausdorff distance measure for face recognition. *Pattern Recogn.* 2007;40(2):431–42.
31. Huttenlocher DP, Klanderman GA, Rucklidge WJ. Comparing images using the Hausdorff distance. *IEEE Trans Pattern Anal Mach Intell.* 1993;15(9):850–63.
32. Sim DG, Kwon OK, Park RH. Object matching algorithms using robust Hausdorff distance measures. *IEEE Trans Image Process.* 1999;8(3):425–9.
33. Shapiro MD, Blaschko MB. On Hausdorff Distance Measures. Amherst: Computer Vision Laboratory University of Massachusetts; 2004. p. 1003.
34. Kwon OK, Sim DG, Park RH. Robust Hausdorff distance matching algorithms using pyramidal structures. *Pattern Recogn.* 2001;34(10):2005–13.
35. Yu CB, Qin HF, Cui YZ, Hu XQ. Finger-vein image recognition combining modified Hausdorff distance with minutiae feature matching. *Interdiscip Sci Comput Life Sci.* 2009;1(4):280–9.
36. Lin KH, Guo B, Lam KM, Siu WC. Human face recognition using a spatially weighted modified Hausdorff distance. In: Proceedings of 2001 International Symposium on Intelligent Multimedia, Video and Speech Processing. ISIMP 2001 (IEEE Cat. No.01EX489). IEEE, 2001. pp. 477–480. <https://doi.org/10.1109/ISIMP.2001.925437>.
37. Zhao C, Shi W, Deng Y. A new Hausdorff distance for image matching. *Pattern Recogn Lett.* 2005;26(5):581–6.
38. Sarangi PP, Panda M, Mishra BSP, Dehuri S. An automated ear localization technique based on modified Hausdorff distance. In: Raman B, Kumar S, Roy P, Sen D, editors. Proceedings of international conference on computer vision and image processing. Advances in intelligent systems and computing, vol 460. Singapore: Springer. https://doi.org/10.1007/978-981-10-2107-7_21.
39. Feng X, Wu W, Li Z, Jeon G, Pang Y. Weighted-Hausdorff distance using gradient orientation information for visible and infrared image registration. *Opt Int J Light Electron Opt.* 2015;126(23):3823–9.
40. Kim J, Kim M, Kim T. Recognition of face orientation angle using modified Hausdorff distance. In: The 18th IEEE International Symposium on Consumer Electronics (ISCE 2014). IEEE, 2014, pp. 1–2. <https://doi.org/10.1109/ISCE.2014.6884449>.
41. Singh N, Pawar S, Kumar Y. Efficient face detection method using modified Hausdorff distance method with C4.5 classifier and canny edge detection. *Int J Comput Appl.* 2015;123(10):38–44. <https://doi.org/10.5120/ijca2015905553>.
42. Rudolph G, Schütze O, Grimme C, Trautmann H. A multiobjective evolutionary algorithm guided by averaged hausdorff distance to aspiration sets. In: Tantar AA, et al. editors. EVOLVE - A bridge between probability, set oriented numerics, and evolutionary computation V. advances in intelligent systems and computing, vol 288. Cham: Springer; 2014. https://doi.org/10.1007/978-3-319-07494-8_18.
43. Chaudhuri BB, Rosenfeld A. A modified Hausdorff distance between fuzzy sets. *Inf Sci.* 1999;118:159–71.
44. Dubuisson MP, Jain AK. A modified Hausdorff distance for object matching. In: Proceedings of 12th International Conference on Pattern Recognition, vol 1. IEEE, 1994. pp. 566–8. <https://doi.org/10.1109/ICPR.1994.576361>.
45. Tian K, Yang X, Kong Q, Yin C, He RL, Yau SST. Two dimensional Yau-hausdorff distance with applications on comparison of DNA and protein sequences. *PLoS One.* 2015;10(9):e0136577.
46. Perona P, Malik J. Scale-space and edge detection using anisotropic diffusion. *IEEE Trans Pattern Anal Mach Intell.* 1990;12(7):629–39.
47. Maiseli B, Msuya H, Kessy S, Kisangiri M. Perona–Malik model with self-adjusting shape-defining constant. *Inf Process Lett.* 2018;137:26–32.
48. Idan M, Speyer JL. Cauchy estimation for linear scalar systems. *IEEE Trans Autom Control.* 2010;55(6):1329–42.
49. Rey WJ. Introduction to robust and quasi-robust statistical methods. New York: Springer; 2012.
50. Ganan S, McClure D. Bayesian image analysis: an application to single photon emission tomography. *Am Stat Assoc.* 1985;12–8.
51. Dennis JE Jr, Welsch RE. Techniques for nonlinear least squares and robust regression. *Commun Stat Simul Comput.* 1978;7(4):345–59.
52. Huber PJ. Robust statistics, vol. 523. New York: Wiley; 2004.
53. Huber PJ. Robust estimation of a location parameter. In: Kotz S, Johnson NL (eds) Breakthroughs in Statistics. Springer Series in Statistics (Perspectives in Statistics). New York, NY: Springer; 1992. https://doi.org/10.1007/978-1-4612-4380-9_35.

54. Chen D. Tukey's biweight estimation for uncertain regression model with imprecise observations. *Soft Comput.* 2020;24:16803–9.
55. Yang G, Li R, Liu Y, Wang J. A robust nonrigid point set registration framework based on global and intrinsic topological constraints. *Visual Comput.* 2021. <https://doi.org/10.1007/s00371-020-02037-7>.
56. Chui H, Rangarajan A. A new point matching algorithm for non-rigid registration. *Comput Vis Image Underst.* 2003;89(2–3):114–41.

Publisher's Note Springer Nature remains neutral with regard to jurisdictional claims in published maps and institutional affiliations.